Kink Formation and Motion in Carbon Nanotubes at High Temperatures

J. Y. Huang,[1,*] S. Chen,[1] Z. F. Ren,[1] Z. Q. Wang,[1] D. Z. Wang,[1] M. Vaziri,[2] Z. Suo,[3] G. Chen,[4] and M. S. Dresselhaus[5]

[1]*Department of Physics, Boston College, Chestnut Hill, Massachusetts 02467, USA*
[2]*Department of Physics, University of Michigan—Flint, Flint, Michigan 48502, USA*
[3]*Division of Engineering and Applied Sciences, Harvard University, Cambridge, Massachusetts 02138, USA*
[4]*Department of Mechanical Engineering, Massachusetts Institute of Technology, Cambridge, Massachusetts 02139, USA*
[5]*Department of Physics and Department of Electrical Engineering and Computer Science, Massachusetts Institute of Technology,
Cambridge, Massachusetts 02139, USA*

We report that kink motion is a *universal* plastic deformation mode in all carbon nanotubes when being tensile loaded at high temperatures. The kink motion, observed inside a high-resolution transmission electron microscope, is reminiscent of dislocation motion in crystalline materials: namely, it dissociates and multiplies. The kinks are nucleated from vacancy creation and aggregation, and propagate in either a longitudinal or a spiral path along the nanotube walls. The kink motion is related to dislocation glide and climb influenced by external stress and high temperatures in carbon nanotubes.

PACS numbers: 61.48.+c, 61.72.Cc, 61.72.Lk, 62.20.Fe

The tensile strength of carbon nanotubes is at least 10 times stronger than that of steel [1–9]. Therefore they are considered to be ideal reinforcement agents to strengthen and toughen ceramics and polymers [10–12]. Despite their important applications, the early theoretical prediction of plasticity in nanotubes has been lacking experimental evidence for almost a decade [13–16]. It was not until recently that plastic deformation in single walled carbon nanotubes was observed experimentally when they were tensile loaded at high temperatures caused by high bias voltages [17]. It was suggested that kink motion might contribute to the superplasticity in single walled carbon nanotubes [17]; however, it was unclear whether kink motion was a *universal* plastic deformation mode in *all* nanotubes. Furthermore, the physics behind the kink motion was not understood. In this Letter, we assert that kink motion was a universal plastic deformation mode in all nanotubes when they were tensile loaded at high temperatures. The multiplication, dissociation, and screw motion of kinks in nanotubes are reported here for the first time. We suggest that kink motion is related to dislocation glide and climb in carbon nanotubes.

Our experiments were conducted inside a high-resolution transmission electron microscope (HRTEM) integrated with a Nanofactory TEM-STM (scanning tunneling microscope) system. The STM probe can be manipulated to contact individual nanotubes in the HRTEM, thus allowing for simultaneous structure and electrical/mechanical property studies [17–19]. Individual single-, double-, or multiwalled carbon nanotube (S/D/MWCNT) sections were produced by electrical breakdown of MWCNTs [18], which were then subjected to tensile-loading experiments at a constant bias voltage [17]. It has been shown that the nanotubes were Joule heated to temperatures higher than 2000 °C at high bias voltages [17–19]. When tensile stressed at such high temperatures,

we discovered kink motion as a universal plastic deformation mode in all kinds of nanotubes including S/D/MWCNTs.

Figure 1 shows kink motion in a SWCNT. The first kink was formed on the upper-right wall, and was then propagated straightly downward with a velocity of 1.7 nm/s, and finally it vanished at the lower-right contact [Figs. 1(a)–1(d), movie M1 [20]]. Just before the vanishing of the first kink, a second kink was formed on the left wall, and migrated progressively downward [Figs. 1(e)–1(h), movie M2 [20]]. Interestingly, the kink was multiplied from one [Fig. 1(e)] to two [Fig. 1(f)] during the propagation, a behavior reminiscent of the dislocation multiplication in crystalline materials [21]. Extremely large kinks were frequently observed [Figs. 1(i) and 1(j)], which appeared to be rather unstable and dissociated into two smaller kinks [Figs. 1(j) and 1(k)], a process analogous to the dissociation of perfect dislocations into partial ones. The sharp kink could not propagate to the lower contacts and was pinned in the middle, leading to early necking and failure of the SWCNT [Fig. 1(m)]. Once a kink was swept by, the diameter of the nanotube was reduced permanently. After successive kink motions, the diameter of the nanotube was reduced from 8.7 nm [Fig. 1(a)] to 1.9 nm [Fig. 1(l)] [22], leading to a continuous current drop (from 100 μA [Fig. 1(a)] to 0 μA [Fig. 1(m)]).

Kink motion was also frequently observed in tensile-loaded DWCNTs (Fig. 2). A kink first was formed near the middle-left wall and was propagated with a velocity of 6 nm/s upward [Figs. 2(b)–2(e)]. Once the kink was swept by, the diameter of the nanotube was reduced instantaneously from 6.45 to 5.85 nm, forming a nanotube junction with the circumference difference between the two constituent nanotubes being 8**b**, where **b** is the magnitude of the Burgers vector $1/3\langle 11\bar{2}0\rangle$ in a graphene sheet. The kink
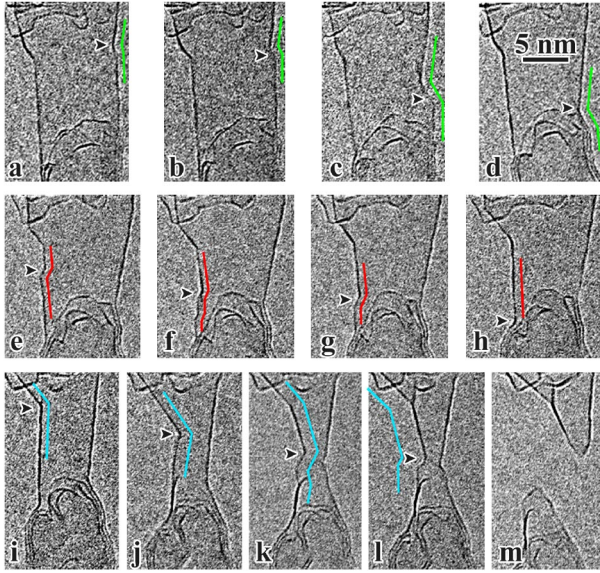
FIG. 1 (color online). Kink motion in a SWCNT. The SWCNT was tensile stressed at 2.8 V bias voltage. The current flowing in the SWCNT was reduced continuously from 100 to 0 μA. The tensile strain was 17%, and the strain rate was 0.02 nm/s. Polarity: positive at the top and negative at the bottom of the SWCNT. Sketches in the figures show the change in the shape and position of the kinks. The velocity of the kink motion ranges from 0.2 to 1.7 nm/s. Arrowheads point to the kinks: (a)–(d) kink motion at the right side of the nanotube wall (movie M1 [20]); (e)–(h) kink motion at the left side of the nanotube wall (movie M2 [20]). In (f), kink multiplication occurred; (i)–(l) motion of a giant kink. The giant kink was dissociated into several smaller kinks in (k) and (l). Necking occurred in (k) and (l), leading to the failure of the carbon nanotube (m).

disappeared after traveling 35 nm along the nanotube walls [Figs. 2(b)–2(f)]. Before the disappearance of the first kink, a second kink was formed on the lower-right walls, and also propagated upward [Figs. 2(e) and 2(f)]. Notably, all the kinks were formed and propagated straightly at the same side of the nanotube walls.

Figure 3 shows kink motion in a MWCNT (movie M3 [20]). A kink was formed on the lower-right wall, and was then propagated upward at a velocity of 0.7 nm/s. Remarkably, after traveling 11 nm, the kink changed its propagation direction from a longitudinal [Figs. 3(a) and 3(b)] to a spiral path [Figs. 3(c)–3(e)] upward, mimicking a screw motion. As it advanced in a spiral path, the kink switched from the right [Fig. 3(c)] to the left wall [Fig. 3(e)]. The kink dissociated into two kinks [Figs. 3(f) and 3(g)] after it moved to the left wall. The two kinks advanced simultaneously upward, but their spacing became shorter. It was also noted that the right side of the innermost wall was detached as the kink advanced. Nevertheless, the kinks moved collaboratively along the different walls.
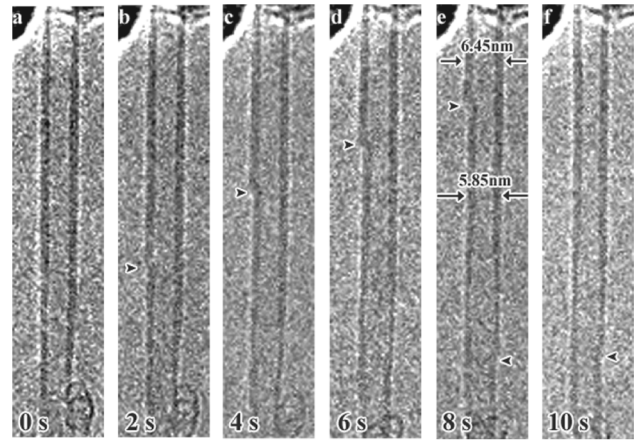

FIG. 2. Kink motion in a DWCNT under tensile stress at 2.3 V and 60 μA. The tensile strain was 10% and the strain rate was 0.7 nm/s. Polarity: positive at top, negative at bottom. Arrowheads point to the kinks. The diameter of the initial DWCNT (a) was uniform. A kink was emitted from the middle-left wall at 2 s (b), and the kink then migrated with a velocity of 6 nm/s upward (c)–(e). A second kink was emitted from the lower-right wall and migrated upward.

The kink-mediated plasticity indicates that nanotubes are ductile at high temperatures. We emphasize the importance of high temperatures on the plastic deformation of nanotubes. We did not observe kink motion in nanotubes when they were tensile stressed at room temperature.

The kink motion can be interpreted in terms of a dislocation mechanism. Each kink is associated with one or several unit dislocations with a Burgers vector of $1/3\langle 1120 \rangle$. A graphene wall of a SWCNT has three sets of crystallogragraphicly equivalent glide planes (B_1, B_2, and B_3 [Fig. 4(a)]). The Burgers vectors of perfect dislocations ($\mathbf{b}_1$, $\mathbf{b}_2$, and $\mathbf{b}_3$ [Fig. 4(a)]) are also located in the three sets of glide planes. The core of a unit dislocation is a $5/7$ pair [Fig. 4(b)]. Such a dislocation was indeed observed by HRTEM recently [23]. When the graphene sheet with an edge dislocation [Fig. 4(b)] is wrapped up, it forms a nanotube junction with the index of the two constituent nanotubes being (n, m) and $(n, m - 1)$ or $(n - 1, m)$, with the extra half lattice plane in the (n, m) nanotube [Fig. 4(c)]. Because the two nanotubes have different diameters, a kink forms in the junction [Fig. 4(c)]. As the Burgers vector of the dislocation is inclined to the tube axis, the kink moves in a spiral path along the nanotube axis. HRTEM images show that most kinks are propagated in a longitudinal direction [Figs. 1, 2, 3(a), and 3(b)] rather than in a spiral path [Figs. 3(c)–3(e)], implying that the motion does not always follow the close-packed planes. Thus the kink motion might occur via a dislocation climb mechanism induced by vacancy diffusion. According to this kink model (Fig. 4), once a kink passes by, the diameter of the nanotube is reduced by a quantum number, and
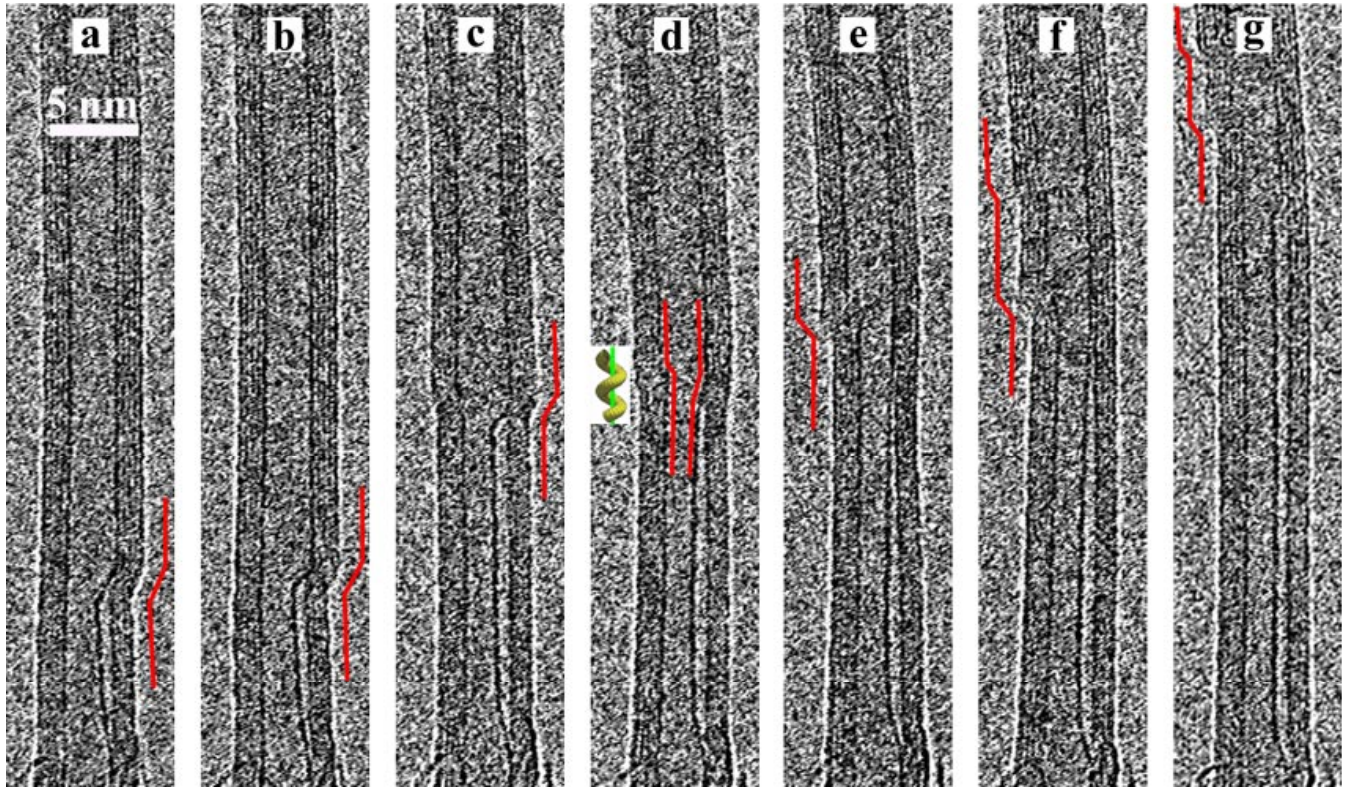
FIG. 3 (color online).   Kink motion in a five-walled nanotube under tensile stress at 2 V and 100 μA (movie M3 [20]). The tensile strain was 3% and the strain rate was 0.04 nm/s. Polarity: positive at top, negative at bottom. The kink was emitted from the lower-right wall (a) and then propagated upward with a velocity of 0.7 nm/s (b),(c). Note that the kink propagation directions changed from a longitudinal (a),(b) to a spiral way upward (c)–(e), as predicted by a dislocation glide mechanism [13–15]. Line sketches highlight the change of kink shapes and positions. The sketch in (d) shows the spiral motion of the kink.

the chiral index of the nanotube is changed from (n, m) to $(n - 1, m)/(n, m - 1)$.

Our observation of kink motion overall is remarkably consistent with Yakobson's theoretical prediction [13–15], in which a Stone-Wales transformation initiates a 5-7-7-5 defect [24], which is the core of a dislocation dipole. Under stress, the two dislocations in the dislocation dipole glide towards opposite directions in a spiral path along the nanotube. However, we also noted two disadvantages in Yakobson's model. First, according to Yakobson's model, one should always observe two kinks moving in the opposite directions simultaneously, which is not consistent with our experimental results showing that only one kink was observed each time. Second, it is difficult to explain the longitudinal kink motion in Yakobson's model. To address the above two issues, our kink model involves only one dislocation, meaning that only one kink should be observed each time, and this feature of our model solves the "two-kink" paradoxes in Yakobson's model. Our model also explains satisfactorily our experimental observations of both the longitudinal and screw motions of kinks, which originate from dislocation climb and dislocation glide, respectively. The problem with Yakobson's model originates from the fact that it neglects vacancy diffusion and

dislocation climb, which dominate the high temperature mechanical behavior of nanotubes, as shown by our experiments.

Vacancies and interstitials are very active at high temperatures, and these defects tend to aggregate to form dislocation loops in a graphene sheet [25–27] and are very likely to aggregate to form a kink in a nanotube. However, the way that the vacancy aggregates differs significantly in graphite from that in nanotubes. Namely, in the former, the vacancies aggregate in the (0002) planes to form dislocation loops with a Burgers vector in the c-axis direction; in the latter, the vacancies aggregate in the (1120) or other prismatic planes to form dislocations with Burgers vectors within the graphene plane (or cylindrical surface of the nanotubes). The reason for the different vacancy aggregation behavior may be attributed to the different experimental conditions. In our experiments, the vacancy diffusion was influenced by the external stress. Once nucleated, the kink was driven to advance by the external stress and high temperatures. Since the atoms around the kink were heavily stressed, they were very likely to evaporate at high temperatures, which then generated vacancy rows around the kink. Atom reconstruction resulted in the advance of the kink. The kink motion
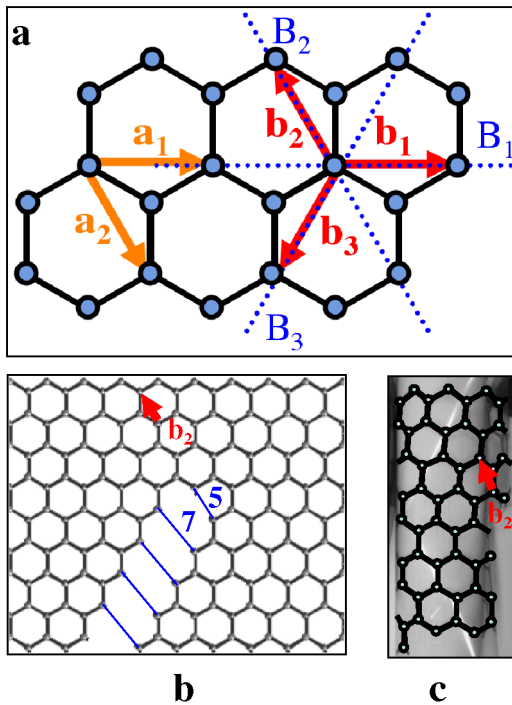
PHYSICAL REVIEW LETTERS

FIG. 4 (color online). (a) The dislocations in a graphite sheet. B_1, B_2, and B_3 are the three sets of glide planes, and $\mathbf{b}_1$, $\mathbf{b}_2$, and $\mathbf{b}_3$ are the Burgers vectors of the three perfect dislocations. $\mathbf{a}_1$ and $\mathbf{a}_2$ are the basis vectors for the (n, m) indexing of the nanotubes. (b) An edge dislocation with a Burgers vector of $\mathbf{b}_2$ in a graphite sheet. The core of the edge dislocation is a 5/7 pair. The edge dislocation was formed by removing half a row of atoms from the graphene sheet. (c) A nanotube junction was formed by wrapping up the graphene sheet in (b). Note the dislocation moves in a spiral way along the nanotube axis, as observed in Figs. 3(c)–3(e) and sketched in the inset of Fig. 3(d).

process was very similar to that of vacancy diffusion driving dislocation climb in crystalline materials. Note that the kink motion was not driven by electromigration or by an electric field, since even under the same polarity in the same tube, we found kink propagation occurring in opposite directions. We thus conclude that the kink motion was driven by high temperatures and external stress.

*Corresponding author.
Electronic address: huangje@bc.edu

[1] T. W. Ebbesen, *Carbon Nanotubes: Preparation and Properties* (CRC Press, New York, 1997).
[2] M. S. Dresselhaus, G. Dresselhaus, and Ph. Avouris, *Carbon Nanotubes: Synthesis, Structure, Properties, and Applications* (Springer, Heidelberg, 2001).
[3] D. Tomanek and R. J. Enbody, *Science and Application of Nanotubes* (Kluwer Academic–Plenum, New York, 2000).
[4] E. W. Wong, P. E. Sheehan, and C. M. Lieber, Science **277**, 1971 (1997).
[5] M. J. Treacy, T. W. Ebbesen, and J. M. Gibson, Nature (London) **381**, 678 (1996).
[6] P. Poncharal *et al.*, Science **283**, 1513 (1999).
[7] B. G. Demczyk *et al.*, Mater. Sci. Eng. A **334**, 173 (2002).
[8] M. F. Yu *et al.*, Science **287**, 637 (2000).
[9] M. F. Yu *et al.*, Phys. Rev. Lett. **84**, 5552 (2000).
[10] R. H. Baughman, A. A. Zakhidov, and W. A. de Heer, Science **297**, 787 (2002).
[11] P. Calvert, Nature (London) **399**, 210 (1999).
[12] G. D. Zhan *et al.*, Nat. Mater. **2**, 38 (2003).
[13] B. I. Yakobson, in *Proceeding of the Recent Advances in the Chemistry and Physics of Fullerenes and Related Materials* (The Electrochemical Society, Pennington, NJ, 1997), Vol. 97, p. 549; Appl. Phys. Lett. **72**, 918 (1998).
[14] T. Dumitrica, M. Hua, and B. I. Yakobson, Proc. Natl. Acad. Sci. U.S.A. **103**, 6105 (2006).
[15] M. B. Nardelli, B. I. Yakobson, and J. Bernholc, Phys. Rev. Lett. **81**, 4656 (1998); Phys. Rev. B **57**, R4277 (1998).
[16] P. H. Zhang, P. E. Lammert, and V. H. Crespi, Phys. Rev. Lett. **81**, 5346 (1998).
[17] J. Y. Huang *et al.*, Nature (London) **439**, 281 (2006).
[18] J. Y. Huang *et al.*, Phys. Rev. Lett. **94**, 236802 (2005).
[19] S. Chen *et al.*, Appl. Phys. Lett. **87**, 263107 (2005).
[20] See EPAPS Document No. E-PRLTAO-97-014634 for *in situ* HRTEM movies showing kink motion. For more information on EPAPS, see http://www.aip.org/pubservs/epaps.html.
[21] J. P. Hirth and J. Lothe, *Theory of Dislocations* (McGraw-Hill, New York, 1968).
[22] The nanotube diameter was not uniform, and we measure the narrowest segment as the diameter for all the nanotubes.
[23] A. Hashimoto *et al.*, Nature (London) **430**, 870 (2004).
[24] A. J. Stone and D. J. Wales, Chem. Phys. Lett. **128**, 501 (1986).
[25] S. Amelinckx and P. Delavignette, Phys. Rev. Lett. **5**, 50 (1960).
[26] F. Banhart, Rep. Prog. Phys. **62**, 1181 (1999).
[27] B. T. Kelly, *Physics of Graphite* (Applied Science, London, 1981).